

## Determination of energy parameters of technology of thermal pore formation

**Pavlenko A.M.**

*Doctor of Technical Sciences  
Professor Department of Building Physics and Renewable Energy  
Kielce University of Technology, Poland,  
E-mail: am.pavlenko@i.ua*

**Shumska L.P.**

*Postgraduate  
Poltava National Technical Yuri Kondratyuk University*

### Abstract

Research porosity thermal insulation of refractory materials is the important task of power engineering, because the thermal conductivity of porous materials depends on the shape and especially location of pore.

Analytical review of existing technologies shows that research in this area is focused on the study of a process separately and generalized theories are not sufficient to clear analysis and model building process heat mass transfer of alumina porous material.

Key words: THERMAL CONDUCTIVITY, POROSITY, SWELLING, HEAT INSULATION

### Introduction

The thermal insulating products are among the most efficient materials for protecting elements of various purposes. Low density, fire resistance, low thermal conductivity and at the same time sufficiently high structural strength allow considering the porous ceramic material as one of the most promising materials for construction [1,2].

It is possible to determine three groups of technologies covering all known methods for obtaining porous structures. In the first group of technologies, the porous structure is created by using artificial or natural pore-forming materials and low-melting clays

via volumetric method or contact concreting – ceramic pores; the second method is the pore forming of slip mass with different ways of foam-forming, dry mineralizing of foam, aeration, low-temperature gas forming; the third method is high-temperature pore-forming of light-alloy raw materials.

Let us consider the third method of structure formation occurring during the hydration of raw material composition [3 - 6].

Carrying out the practical research into raw mass, we added the chamotte clay or pure structural clay, the composition of which is shown in the Table 1.

**Table 1.** The chemical composition of fire-clay

Clay	The content of oxides, %									
	SiO <sub>2</sub>	Al <sub>2</sub> O <sub>3</sub>	Fe <sub>2</sub> O <sub>3</sub>	TiO <sub>2</sub>	CaO	MgO	K <sub>2</sub> O	Na <sub>2</sub> O	SO <sub>3</sub>	Lost on ignition
Structural clay	44.59-54.14	27.13-35.85	1.48-2.47	1.14-1.97	0.38-0.81	0.23-0.42	0.21-0.60	0.25-0.45	1.34-3.62	11.48-13.86
Chamotte clay	46.80	36.80	1.58	-	0.20	0.76	0.34	0.18	-	13.6

The research objective is to determine the optimal ratio of additives' masses in accordance with energy consumption to implement the thermal bloating process, strength of the obtained material, porosity and thermal conductivity.

Obviously, thermal conductivity and energy consumption should be minimal.

The research was performed by the use of differential thermal analysis (DTA) of the thermal bloating

process for the raw mixture.

Trails are performed at a constant rise of temperature with recording the temperature difference on the chart paper as a function of temperature. The result is a curve DTA (Fig. 1-4). At processing the experiment's results, the horizontal axis should be graded by temperature. According to the position of peak of the endothermic process, the temperature interval of phase transitions can be found.

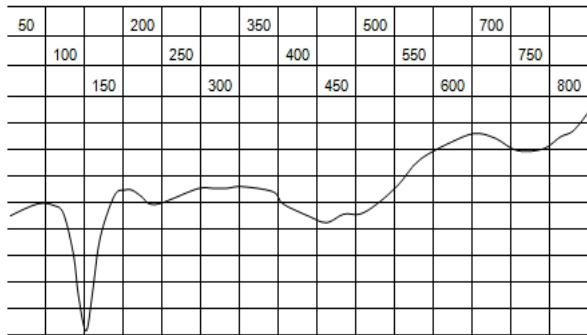


**Figure 1.** DTA of raw material mixture with a content of 75 mass fractions of clay No 1 (Table 1)

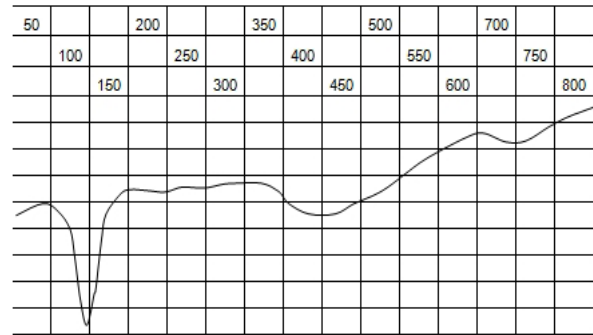


**Figure 2.** DTA of raw material mixture with a content of 75 mass fractions of clay No 2 (Table 1)

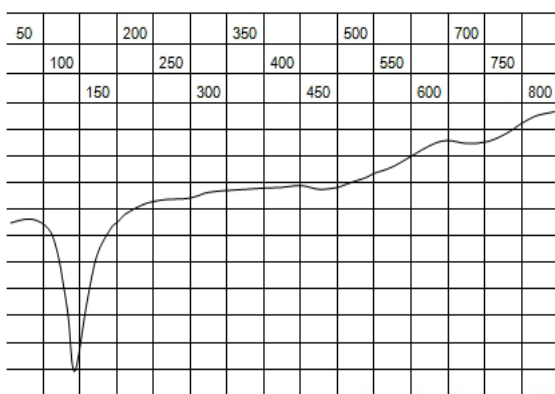


**Figure 3.** DTA of raw material mixture with a content of 160 mass fractions of clay No 1 (Table 1)

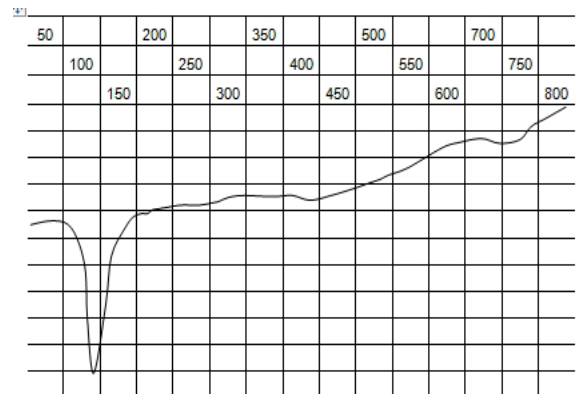


**Figure 4.** DTA of raw material mixture with a content of 160 mass fractions of clay No 2 (Table 1)

There is no significant difference in thermal evidence of phase transformations of clays of samples No 1 and No 2 in the charts. However, at increasing the alumina content, the exotherm of moisture removal has a higher minimum, which is a consequence of

higher water saturation of the raw material mixture.

On DTA curves the low-temperature endothermic peak of 146 °C is recorded, which is due to the removal of adsorbed water; the presence of water is caused by high specific surface area of particles that is direct-

ly dependent on disorder of mixture.

Changes, which took place during the heating, showed three endothermic effects: 146, 500, and 720 (average temperature intervals in Fig. 1-4). A large endothermic effect due to the removal of absorbed water is observed at 146 °C, and the step observed on the curve at 300 °C indicates removal of interpacket water. The second effect (450-550 °C) corresponds to the removal of the constitutional water (bound into the form of OH). The endothermic effect at 720 °C explains the removal of OH-ions. As it can be seen from the data chart, the optimum temperature range for dehydration of the mixture is within 146-720 °C. It should be defined the connection of temperature intervals with the structure of bloated material, and, consequently, with the useful application properties (strength, conductivity, heat resistance, water absorption). For this, changing the composition of the initial mixture, the measurements were repeated under method presented above.

In the obtained DTA curves for all experimental samples in the investigated temperature intervals, a number of phenomena associated with thermal effects are observed: 1) up to 100 °C — evaporation of chemically unbound water; 2) 100...170°C — a sudden loss of mass and strongly expressed endothermic effect that is related to the partial dehydration of gel and phases of different composition; 3) 450...550 °C — endothermic effect that corresponds to the decomposition of portlandite with water vapor emission 4) 700...900 °C — a minor loss of mass and weak endothermic effect, which is related to the decomposition of carbonate minerals (calcite, dolomite), and late-stage dehydration of gel and hydro aluminates.

### Studies of the pore structure

The morphology and porosity of the samples were determined by optical methods. According to this method, the macroscopic parameters of porosity inside metric interval with a lower bound of 10 mμ and upper bound of 5 mm are determined. The specified interval characterizes the strength parameters of the substance and parameters of heat and mass transfer.

To analyze the structure a polished thin section of bloated material was made and preliminary analysis was carried out at the installation consisting of a projection optical system, television camera and computer with the interface. The general view of thin section in visible light in gray with 256 shades of gray was recorded at 10-times increase. Visualization of pores was carried out by methods of shadow contrast, which is based on applying a system of lighting the surface of a sample, which consists of lights directed at small angles to the surface. When using the method of luminous contrasting the luminophore layer was applied on the surface of the thin section. Thickness of luminophore was preliminary rated by the method of water sedimentation with reveal of luminophore particles of submicron size. Excess luminophore is removed from the surface by blowing, after what a specialized film is applied on the surface to remove the remaining luminophore particles. The sample's surface was controlled via a binocular microscope. In the plane of granules and inter-granules planes the pores with a minimum size of 150 mμ were recorded. The object marker lay-out defined by the contours of particles of the fired granules was built. The resulting scene is analyzed with determining the size (Fig. 5-10).

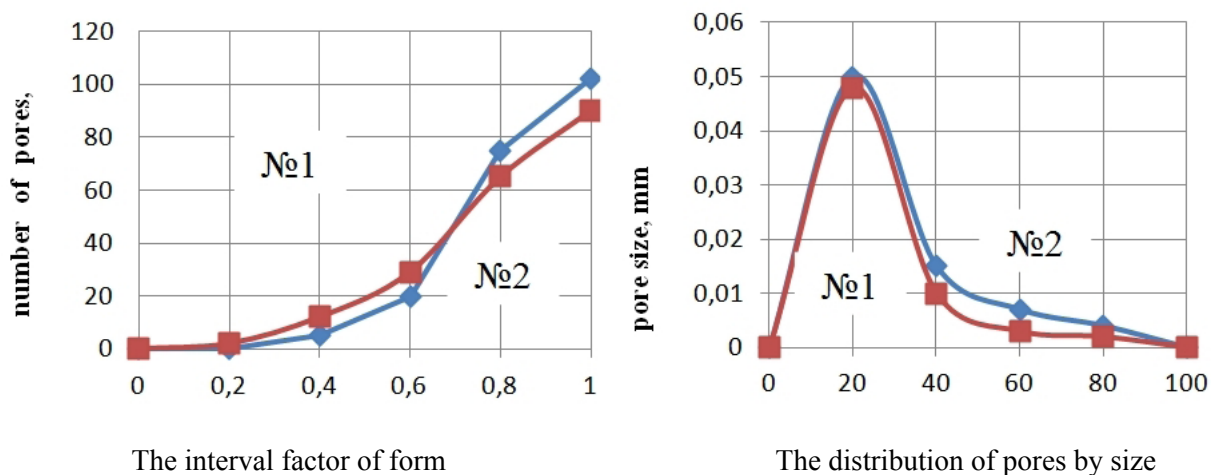
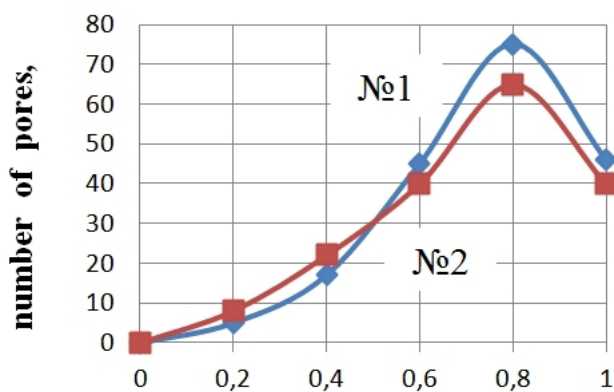
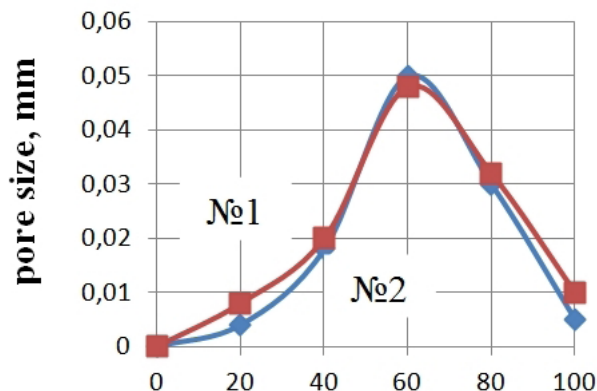


**Figure 5.** The parameters of total porosity of the samples No 1 and No 2 (75 mass fractions) bloated at temperature of 160 °C (the first endothermic minimum)

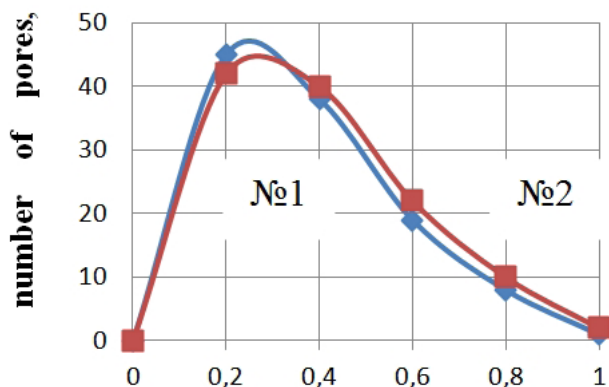


The interval factor of form

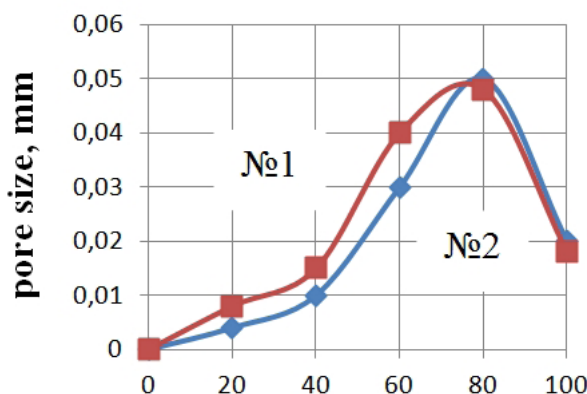


The distribution of pores by size

Figure 6. The parameters of total porosity of the samples No 1 and No 2 (75 mass fractions) bloated at temperature of 300 °C (the first endothermic minimum)

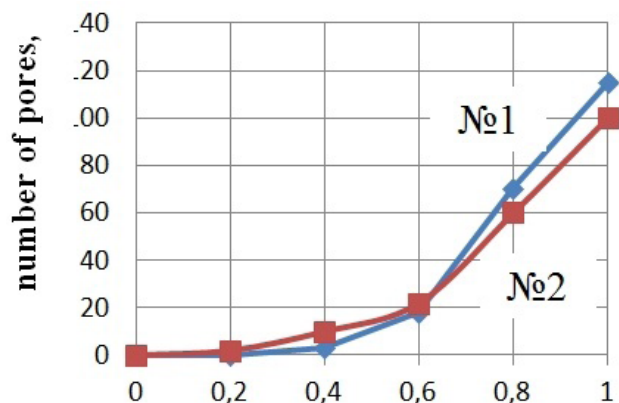


The interval factor of form

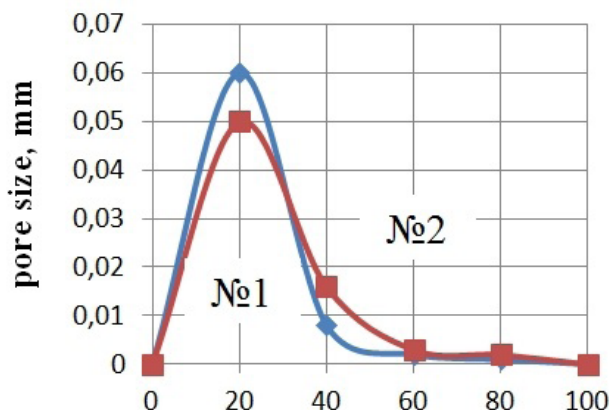


The distribution of pores by size

Figure 7. The parameters of total porosity of the samples No 1 and No 2 (75 mass fractions) bloated at temperature of 700 °C (the first endothermic minimum)



The interval factor of form



The distribution of pores by size

Figure 8. The parameters of total porosity of the samples No 1 and No 2 (160 mass fractions) bloated at temperature of 160 °C (the first endothermic minimum)

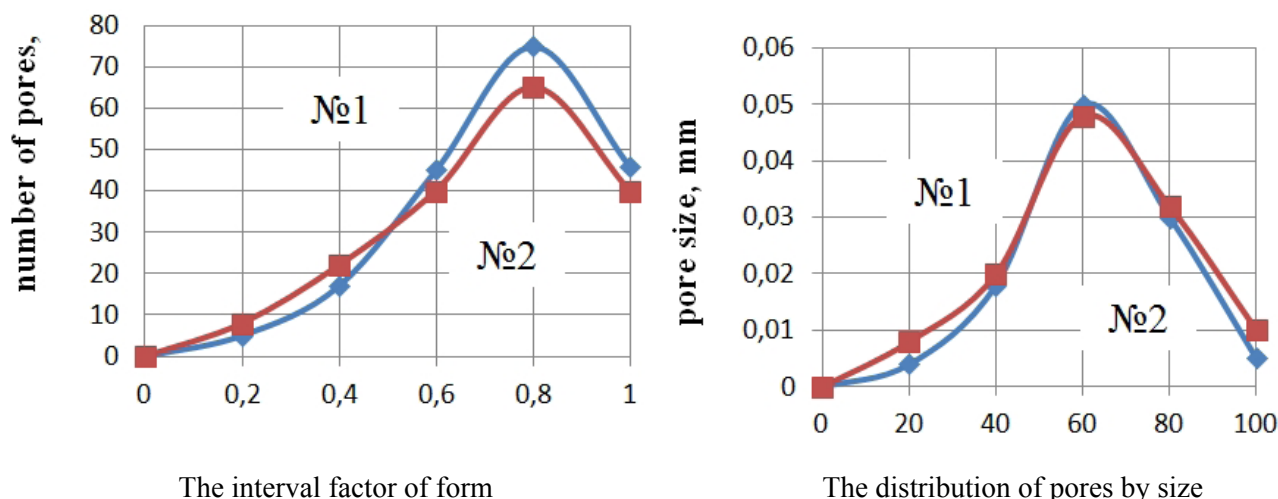


Figure 9. The parameters of total porosity of the samples No 1 and No 2 (160 mass fractions) bloated at temperature of 300 °C (the first endothermic minimum)

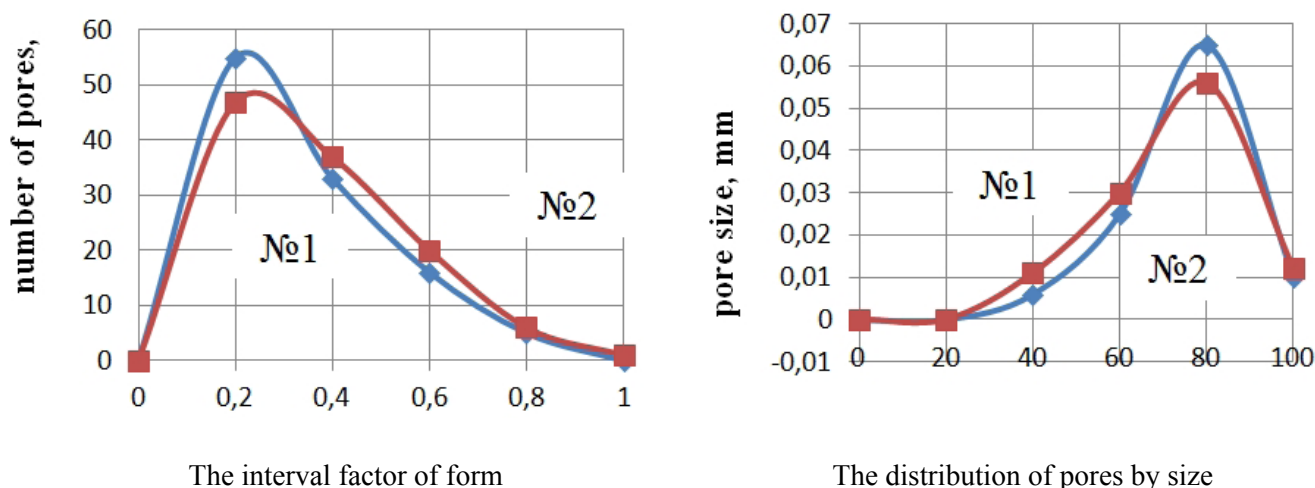


Figure 10. The parameters of total porosity of the samples No 1 and No 2 (160 mass fractions) bloated at temperature of 700 °C (the first endothermic minimum)

In figures 5-10, the porosity parameters of samples No 1 and No 2 for the mixture with different content of 75 and 160 mass fractions are shown. The characteristic feature of the obtained data is that graphs for different types of clay are almost the same. Significant differences are in reading for different temperature minimums. So, for the first endothermic minimum, we obtained the bloated material with small and almost spherical pores [7-9]. Most of them had a minimum size. The bloating of the raw material mixture in the second endothermic minimum provides a mixed porosity (spherical cellular and channel). The material becomes less solid. When there is bloating in the conditions of the third endothermic minimum the channel porosity is mainly formed. This material has the lowest strength. The reducing in thermal conductivity with increasing temperature of bloating should be expected.

### Conclusions

The solution of task of creating new porous thermal insulation materials and technologies of their production is inextricably related to scientific research in energy transferring of porous structure during the stages of bloating, hardening and drying under the condition of providing the lowest thermal conductivity and density.

The indicated material properties are determined by a rate of their porosity, the ratio of micro and macro porosities, properties of interporous material that form a kind of supporting structure, which in its turn is determined by the production technology, type of raw materials and conditions of their preparation. All mentioned above impose the special requirements to the formation of material structure to ensure its relatively high strength and durability.

With the help of differential thermal analysis, the

modes of heat treatment have been studied; the rational parameters of thermal bloating has been defined that allows to implement the process with minimal energy consumption with predicted thermal properties of obtained materials.

### References

1. Pavlenko A., Koshlak H. (2015) Design of processes of thermal bloating of silicates. *Metallurgical and Mining Industry*. No 1, p.p.118-122.
2. Eom, J.-H., Kim Y.-W., Raju S. (2013) Processing and properties of macroporous silicon carbide ceramics: A review. *Journal of Asian Ceramic Societies*. Vol. 1, No 3. p.p. 220–242.
3. Komissarchuk O., Xu Z., Hao H. (2014) Pore structure and mechanical properties of directionally solidified porous aluminum alloys. *China Foundry* (electronic source). Vol. 11, No 1. p.p. 1–7. Available at: <https://doaj.org/article/002c72e2e01345db8bf4fef190113057>.
4. Bajare D., Kazjonovs J., Korjakins A. (2013) Lightweight Concrete with Aggregates Made by Using Industrial Waste. *Journal of Sustainable Architecture and Civil Engineering*. Vol. 4, No 5.
5. Lopez-Pamies O., Ponte Castaneda P., Idiart M. I. (2012) Effects of internal pore pressure on closed-cell elastomeric foams. *International Journal of Solids and Structures*. Vol. 49, No 19-20. p.p. 2793–2798.
6. Gunasegaram D. R., Farnsworth D. J., Nguyen T. T. (2009) Identification of critical factors affecting shrinkage porosity in permanent mold casting using numerical simulations based on design of experiments. *Materials Processing Technology*. Vol. 209, p.p. 1209-1219.
7. Grunsven W. (2014) Porous metal implants for enhanced bone ingrowth and stability. *Thesis submitted to the University of Sheffield for the degree of Doctor of Philosophy. Department of Materials Science and Engineering*. September 2014.
8. Lepeshkin I. A., Ershov M. Ju. (2010) Vspenennyj aluminij v avtomobilestroenii [The foam aluminum in automotive industry]. *Avtomobil'naja promyshlennost'* [Automotive industry]. No 10, p.p. 36-39.
9. Krushenko G. G. (2012) Poluchenie i primenenie poristyh metallicheskih materialov v tehnike [Obtaining and application of porous metal materials in the technique]. *Vestnik Sibirskogo gosudarstvennogo ajerokosmicheskogo universiteta imeni akademika M. F. Reshetneva. Tehnologicheskie processy i materialy*. [Journal of Siberian State Aerospace University. Technological processes and materials]. p.p. 181-184.

## Metallurgical and Mining Industry

[www.metaljournal.com.ua](http://www.metaljournal.com.ua)